



HAL
open science

Experimental Analysis of Micromilling Cutting Forces on Super Duplex Stainless Steel ICOMM 2014 No

Anna Carla Araujo, Adriane Lopes Mougo, Fábio Oliveira Campos

► To cite this version:

Anna Carla Araujo, Adriane Lopes Mougo, Fábio Oliveira Campos. Experimental Analysis of Micromilling Cutting Forces on Super Duplex Stainless Steel ICOMM 2014 No. International Conference on Micro Manufacturing ICOMM 2014, 2014, Singapour, Singapore. hal-03219974

HAL Id: hal-03219974

<https://hal.science/hal-03219974>

Submitted on 6 May 2021

HAL is a multi-disciplinary open access archive for the deposit and dissemination of scientific research documents, whether they are published or not. The documents may come from teaching and research institutions in France or abroad, or from public or private research centers.

L'archive ouverte pluridisciplinaire **HAL**, est destinée au dépôt et à la diffusion de documents scientifiques de niveau recherche, publiés ou non, émanant des établissements d'enseignement et de recherche français ou étrangers, des laboratoires publics ou privés.

Experimental Analysis of Micromilling Cutting Forces on Super Duplex Stainless Steel

ICOMM
2014
No.

Adriane Lopes Mougo, Fabio de Oliveira Campos and Anna Carla Araujo

Mechanical Engineering Department, COPPE/UFRJ, Brazil; anna@ufrj.br

Abstract

Technological development has required the fabrication of miniaturized components in different industry areas, such as electronics, aerospace, automotive, medical and biotechnology. Micromilling aims to produce micro parts with new applications, high performance and quality, requiring production conditions favorable for surface integrity of the workpiece and the useful life of the tool. Super duplex UNS S 32750 stainless steel is used in chemical process pressure vessels, piping and heat exchangers, offshore oil production/technology, oil and gas industry equipment and it is known to have two phases with relevant differences concerning mechanical properties. There are not many studies on micromachining of superduplex components. This article presents an experimental study of micromilling UNS S 32750 workpiece. The design of experiments (DOE) uses two levels of feed per tooth and cutting velocity to analyze the resultant cutting forces. The increase of feed per tooth decreased the specific cutting pressure and higher cutting speeds caused lower specific cutting pressures. For the lower feed per tooth, stronger variation of the force peaks was noted, that could indicate the passage of each tooth in different phases.

Keywords: Micromilling, Super duplex, cutting forces.

1. Introduction

The size of the part in machining of metallic components plays an important role in the force prediction. The mechanisms between macro and microcutting can be different due to the substantial size reduction. This is known as "size effect" in micromachining [1]. Feed per tooth to tool radius ratio has to be higher than in conventional milling to keep productivity at a reasonable level [2]. Due to the small size of the microtools, which have a diameter of less than 2 mm, it is very difficult to notice the damage in the cutting edges and an inappropriate selection of the cutting conditions can cause tool breakage unexpectedly.

When the relationship between the main geometrical features is kept constant, the process behaviour changes. Vollertsen et al. [3] presented a review on the typology of size effects, a description of size effects on strength and tribology and size effects on formability and machinability. Camara et al. [4] presented a state of art on micromilling with emphasis on the work material requirements, tool materials and geometry, cutting forces, temperature, quality of the finished product, burr formation, process modelling and monitoring and machine tool requirements. Afazov et al. [5] studied the micromilling conditions on the cutting forces and process stability through the effects of the tool wear, rake angle, run-out and workpiece material.

At low feed rates, when chip thickness (t_c) is lower than the required minimum chip thickness (t_{cmin}), rubbing or ploughing occurs instead of cutting [6]. A critical cutting thickness needs to be exceeded to promote the chip removal. Ramos et al. [7] studied the

transition from ploughing to cutting in micromachining and evaluated the minimum uncut chip thickness. In this study the changes of the surface roughness, surface topography and residual stress state after microcutting have been also investigated. If the chip thickness is below this value ($t_c < t_{cmin}$), the ploughing mechanism is present, where part of the material is plastically pushed against the workpiece surface.

It is also possible to have the elasticity mechanism when the forces are lower. In this case, $t_c \ll t_{cmin}$ and the forces are proportional to the interference volume between the tool and the workpiece [8]. Similarly, Malekian et al. [9] used the minimum uncut chip thickness, under which the material is not removed but ploughed, and claimed that this effect causes an increase of machining forces which affect the surface integrity of the workpiece.

Microstructure has also a significant effect on microscale cutting. Simoneau et al. [10] investigated the effect of grain size and orientation during microcutting in FE modelling of the primary shear zone. Their research group [11] analyzed the orthogonal cutting in microscale. Tests were conducted on steel and the resulting chips examined showing that the chip formation changes from continuous to "quasi-shear-extrusion" chip due to the uncut thickness size. The results indicate that the pearlite and softer ferrite grains play distinct roles in the plastic deformation process.

Literature review shows the assumption of non-homogeneity in workpiece material properties because the micro-grain-structure size is of the same order of magnitude as the cutter radius of curvature and the grain structures will affect the cutting properties [1, 5, 10].

Between the most studied materials in machining

and micromachining process has duplex and super duplex steels. Super duplex steels have a two-phase structure containing ferrite and austenite in almost equal proportion and these materials are important for use in offshore platforms in applications that involve pumping of produced water. The most common problem of this material is the cold hardening process experienced by the metal structure after plastic deformation, which can occur in the machining process. The increase in the surface hardness can cause increased shearing forces necessary to remove the chip in micromachining process, influencing the quality of the workpiece and in the tool wear.

Super duplex UNS S 32750 is an extremely corrosion-resistant alloy developed to work in very demanding applications, in which the workpieces are exposed to corrosive environments. Their chemical composition and microstructure (high molybdenum, chromium and nitrogen content) cause high resistance to chloride pitting and crevice corrosion attack, but the machinability of these alloys is generally poor and results in long production cycles and high tool costs.

This article presents an experimental study on micromilling super duplex stainless steel using different feed per tooth and cutting velocity aiming to calibrate a model for estimation of the specific pressure and variation in cutting force due to the bi-phasic microstructure of the steel.

2. Cutting Force Modelling

2.1. Chip load Cutting model

Elemental normal and frictional forces are required to the determination of cutting forces for a given geometry. The mechanistic modeling approach is a combination of analytical and empirical methods in which the forces are proportional to the chip load [12].

The specific cutting pressure, K_n , K_f and K_z (tangential, radial and axial coefficients respectively), have been shown as a function of chip thickness t_c in mesoscale milling process and it is used for calculation of dF_n , dF_f and dF_z on each angular position θ of the discretized cutting edge proportional to the chip load area dA (see Eq. 1).

$$\begin{aligned} dF_n(\theta) &= K_n dA(\theta) \\ dF_f(\theta) &= m_1 K_f dA(\theta) \\ dF_z(\theta) &= m_2 K_z dA(\theta) \end{aligned} \quad (1)$$

Using a semi empirical modeling as [13], relating specific cutting pressures by empiric factors m_1 and m_2 . Chip area is calculated based on uncut chip thickness $t_c(\theta)$, that is called Martellotti equation, (see Eq. 2):

$$t_c(\theta) = f_i \sin(\theta) \quad (2)$$

The specific cutting pressure (K_i) is calculated using mechanistic relation, as a function of feed per tooth and cutting velocity:

$$\ln K_i = a_0 + a_1 \ln t_c + a_2 \ln V_c + a_3 \ln(t_c V_c) \quad (3)$$

The coefficients a_0 , a_1 , a_2 and a_3 are called specific cutting energy coefficients. They are dependent on the

tool and workpiece materials and also on the cutting speed and the chip thickness. They are determined from calibration tests for a given tool work piece combination and for a given range of cutting conditions.

2.2. Chip thickness correction in micro cutting model

Bao and Tansel [2] developed a more precise expression than Martelotti calculation for uncut chip thickness $t_c(\theta)$ used by Newby et al. [14] to calculate average uncut thickness (see Eq. 4).

$$t_c(\theta) = f_i \sin(\theta) - \frac{z}{2\pi r} f_i^2 \sin(\theta) \cos(\theta) + \frac{f_i^2}{2f} \cos^2(\theta) \quad (4)$$

Where z , n and r are the tool teeth, spindle speed and tool radius respectively.

Ploughing effect occur under minimum uncut chip thickness, which was modeled by different approaches. Liu et al. [15] modeled considering analytical model using slip line theory and Johnson-Cook model. Malekian et al. [9] presented an article on micromilling of aluminum, which is used in this article based on the edge radius r_e and on a critical or stagnant angle, Φ_m , equal to the friction angle between the material and the rake face, regardless of the other parameters involved in the process (see Eq. 5).

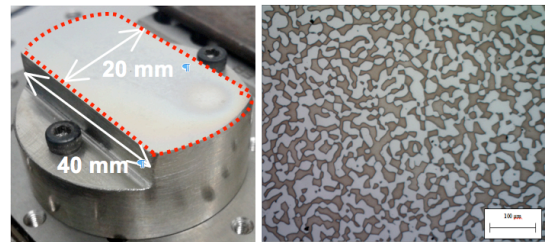
$$t_{cm}(\theta) = r_e (1 - \cos(\phi_m)) \quad (5)$$

3. Experimental setup

Aiming to analyze the cutting forces and the influence of the microstructure of the material on them, a series of experiments will be performed.

3.1. Material and experimental apparatus

The super duplex stainless steel (USS 32750) workpiece dimension presents an useful area for micro machining of 40mm x 20mm, presented in Fig. 1 (a), and it has an heterogeneous microstructure, as seen in Fig. 1 (b).



(a) workpiece material (b) microstructure
Fig. 1. Super duplex stainless steel (UNS S 32750)

The microstructure obtained from the work surface of the piece does not show well-delimited grain contour. Therefore, it was not possible to measure the average grain diameter. So, after the metallographic preparation, the images were analyzed in the Image-Pro Plus software in order to quantify the volumetric fraction of the ferrite, dark grains in Fig.1b, (52%) and austenite (48%) phases.

A carbide micromilling tool is used and its diameter is 0.8 mm, Fig. 2, with two flutes. This micro mill material is Tungsten Carbide-Cobalt (WC/Co) and the

cutting length is coated with Titanium aluminum nitride (TiAlN-F) with thin particles, Fig. 3.

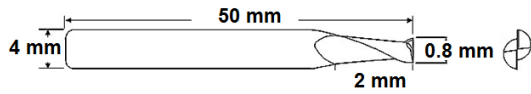


Fig. 2. Dimensions of the micro milling tool.

This tool is indicated to operations in steels with hardness greater than 48 HRC. Therefore, it was executed a micro hardness test on the workpiece surface as new. The test consisted of the application of 1 Kg load during approximately 30 s. The micro hardness average found was 346 HV, that is, 35 HRC, according to the conversion table.

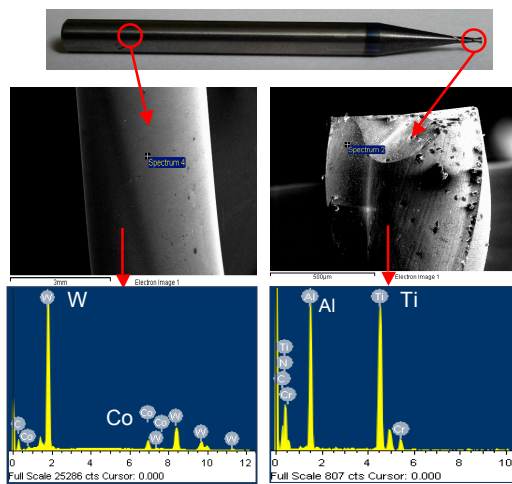


Fig. 3. SEM Microscopy and EDS of Micro milling tool

The micro machine tool that is used on the experiments is the CNC Mini Mill/GX from Minitech Machinery Corporation. The machine uses NSK 60k RPM precision spindle with 3-axis controller. Its standard resolution is 0.78125 μm using dual linear ball bearing slides on each axis, sealed for the table mechanism (THK linear slides - RSR15 series, caged-ball technology). The drive mechanism THK Ball Screw actuator - preloaded and sealed, achieves low torque fluctuation and no backlash.

A minidynamometer has been used for cutting force measurement: the MiniDyn 9256C2 from KISTLER with cable 1697A5. It was used a charge amplifier 5070A10100 and a data acquisition board NI USB 6251, from National Instruments. The minidynamometer was calibrated with a sensitivity of -25.61 pC/N on F_x , -12.68 pC/N on F_y and -25.86 pC/N on F_z . An overview of the equipment that was used can be seen in the Table 1.

Table 1

Equipment specifications for force acquisition

Equipment	Specification
Micro Machine	Mini-Mill GX
Charge Amplifier	Kistler 5070A10100
Acquisition Plate	National Instruments USB 6251
Dynamometer	Kistler MiniDyn 9256C2

3.2. Experimental Procedure

Before the actual micromilling experiments started, a surface of 40 x 20 mm, the work area, was faced on the workpiece using a 3 mm milling tool and the perpendicularity of the milling axis regarding the milling surface was checked with a dial indicator. It was used 50 m/min as cutting velocity, feed rate equals to 100 mm/min and 0.1 mm depth of cut. The face milling operation is important because it ensures that the micromilling operation would be performed on a flat surface. If the surface to be machined was not flat, the axial depth of cut could vary during the cutting process and the forces data would not be right.

The experiments were planned to analyze the influence of two factors, with two levels each, on the cutting force. The factors chosen were the feed per tooth and the cutting velocity and three replicates for each experiment. It was used clockwise spindle speed and cutting fluid (Microcut 510F Quaker). Table 2 presents the cutting parameters used on the experiments.

Table 2

Cutting data

Data	Values
Spindle speed (n)	12000 rpm and 20000 rpm
Feed per tooth (ft)	7 $\mu\text{m}/\text{th}$ and 10 $\mu\text{m}/\text{th}$
Depth of cut (ap)	100 μm
Tool	Tungsten carbide, d=0,8mm
Workpiece	Super duplex UNS S 32750

The Table 3 presents the cutting parameters used in each experiment, 3 replicates each. The order of the tests was planned in a way to ensure the randomization of them.

Table 3

Cutting parameters for each experiment and replicates.

Exp.	Tests	Vf (mm/min)	n (rpm)
1	5, 6 and 11	280	20000
2	1, 3 and 8	168	12000
3	4, 7 and 9	400	20000
4	2, 10 and 12	240	12000

4. Results and discussions

In this section, it is presented the experimental data and the calculation of basic specific cutting pressure.

4.1. Experimental results

The total length of the micro milled channels was approximately 3 mm for all the tests. In order to secure the cutting force signal acquisition, the tool was positioned out of the piece around 10 mm, in the opposite sense of the feed direction.

For all the experiments, it was possible to observe the signal acquisition (noises) during the tool displacement, as presented in Fig. 4.

This noise can be directly related to the machine rigidity and with the run-out of the tool rotational axis. The run-out occurs when the tool axis is not perfectly aligned with the tool chuck or with the mill fuse.

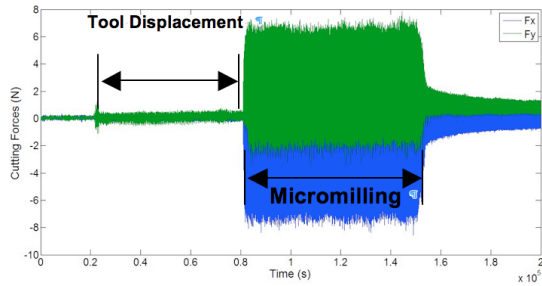
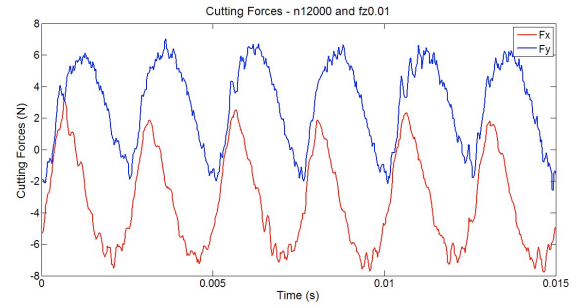


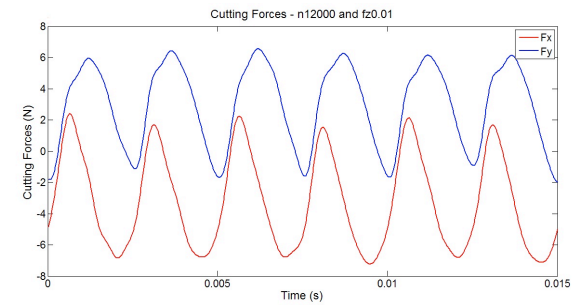
Fig. 4. Experimental cutting forces for experiment 4.

The signals were filtered using a low-pass filter with the cut-off frequency corresponding to the frequency of the spindle speed. As it was noticed in the Fig. 4 even when the tool is not cutting, there is a smaller signal due the feed and the spindle on.

Figure 5 shows the original and the filtered cutting force signals for three tool revolutions of the experiment 4. It is possible to observe a low noise level interfering during the signal acquisition. Using a low-pass filter with cut-off frequency of 2 KHz, it is possible to remove these noises without affecting the cutting force profile significantly.



(a). Experiment 4: unfiltered signal.



(b). Experiment 4: filtered signal.

Fig. 5. Experimental cutting forces for 6 teeth passes

To analyze the signal, one representative vector for cutting was generated using points calculated by the average cutting data of twenty revolutions of the tool. The method for the compute of this average is presented in the Fig. 6 and by the Eq. 6 and Eq. 7. The result of this average for each experiment is showed in Fig. 7.

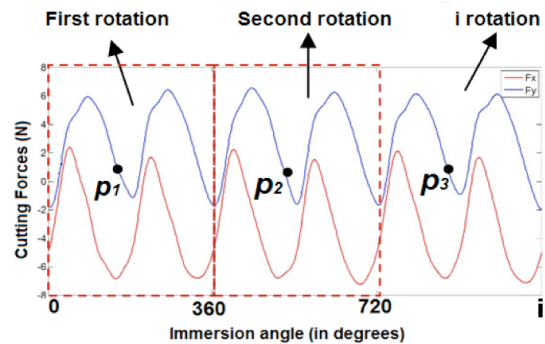


Fig. 6. Method to calculate the representative cutting force data for each experiment.

With the spindle speed (n) and the signal acquisition frequency (f_A), is possible to compute the quantity of points (p) in the XY coordinate that constitute a complete revolution (see Eq. 6).

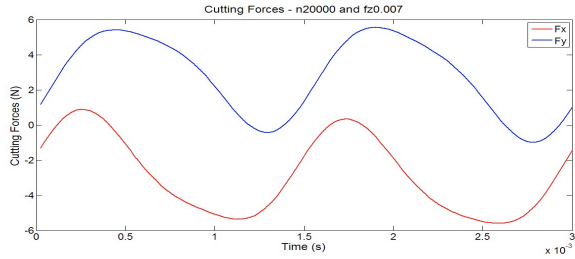
$$x = \frac{n}{60s} \cdot \frac{1}{f_A} \quad (6)$$

For values of f_A equal to 40.000 Hz, the quantity of points in a revolution, in relation to cutting speeds of 30 m/min and 50 m/min, is 200 and 120 points,

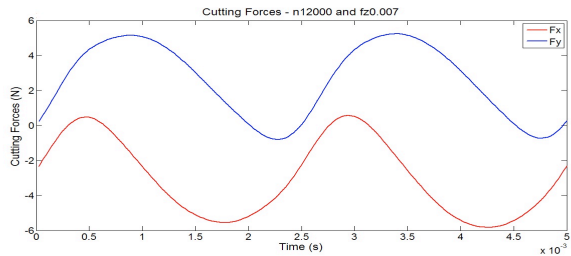
respectively (see Eq. 7).

$$F_{xy}(p) = \sum \frac{f_i(p + p.i)}{20} \quad (7)$$

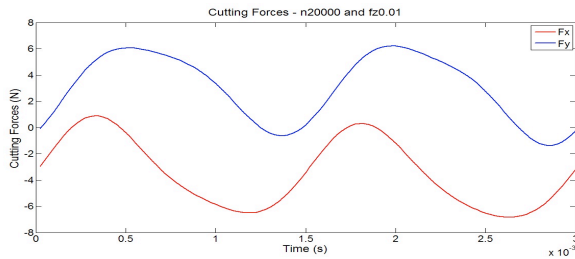
For $i=0, \dots, 19$.



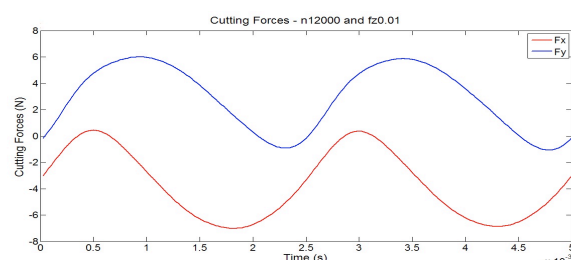
(a) Experiment 1.



(b) Experiment 2.



(c) Experiment 3.



(d) Experiment 4.

Fig. 7. Average of twenty rotations of the tool.

The maximum resultant force of each revolution was calculated. An average of the 20 maximum forces was identified, so the resultant cutting pressure can be computed.

4.2. Specific cutting force

Using the experimental results of Malekian et al. [9], m_1 and m_2 on Eq. 1 are 0.6 and 0.2, respectively it is possible to calculate tangential and radial cutting pressures. Using the average maximum force and the maximum chip area - feed times depth of cut - the resultant cutting pressure can be calculated. The

experimental specific cutting pressure for each experiment is given by Eq. 8.

$$K_t = \frac{K_{res-max}}{\sqrt{1 + 0.6^2 + 0.2^2}} \quad (8)$$

Using Eq. 3 and computing the experimental specific cutting pressure, the coefficients a_0 , a_1 , a_2 and a_3 can be calculated by solving a linear system. The mechanistic function for specific cutting pressure can be developed and the results, using cutting parameters, can be compared with the experimental data. The experiments 1, 2, 3 and 4 were used to calibrate the model. After solving the linear system, Eq. 3 becomes (see Eq. 9):

$$\ln K_t = 6.8329 - 0.3128 \ln t_c + 0.0965 \ln V_c - 0.2163 \ln(t_c V_c) \quad (9)$$

The errors between the experimental specific cutting pressure and the numerical specific cutting pressure are shown in Tab. 4.

Table 4
Experimental and numerical K_t

Experiment	Experimental (MPa)	Numerical (MPa)	Error (%)
K_{t1}	7968.6	8015.8	0.59
K_{t2}	8572.3	8521.8	0.58
K_{t3}	6676.7	6637.4	0.58
K_{t3}	7014.8	7056.3	0.59

Using all maximum resultant forces, all experiments and replicates, it is possible to make an statistical analysis. Figure 8 presents the effect of feed per tooth and cutting velocity on the specific cutting pressure.

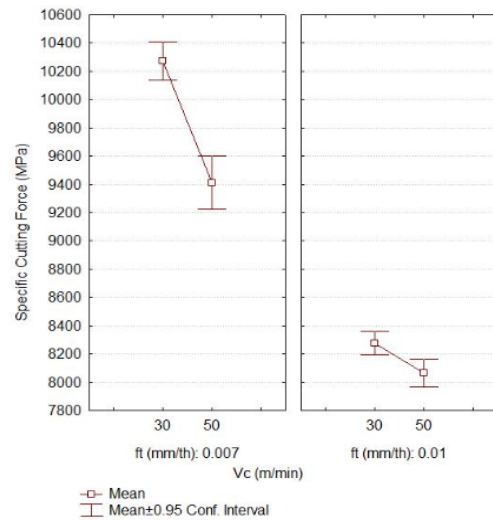


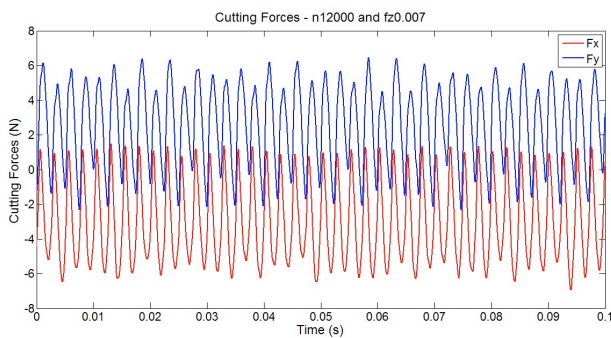
Fig. 8. Effect of feed per tooth and cutting velocity on specific cutting pressure.

The results show that, for both levels of the cutting speed, a lower feed per tooth produce higher specific

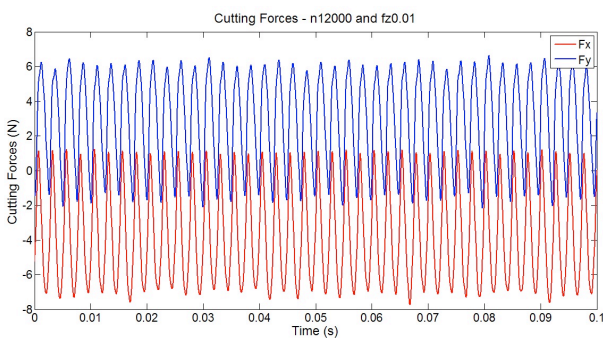
cutting pressure, because of the smaller quantity of material removed. For both values of feed per tooth, an increase in the cutting speed decreased the specific cutting pressure. It is possible to observe, also, that the standard deviation of the specific cutting pressure is bigger for the experiments executed with feed per tooth equal to 0.007 mm/th.

Although it was not possible to determine the average grain diameter, it is clear that a lower feed rate on the work surface, greater will be the cutting force variation, caused one time by the passage of the tooth in the ferrite phase and another by the passage of the tooth in the austenite phase.

Figure 9 shows twenty tool revolutions of the test 8 (0.007 mm/th) and test 2 ($f_z=0.01$ mm/th) aiming to present the variation of peaks of the maximum cutting force, which are used to compute the experimental specific cutting pressure. It can be seen that on Fig.9a the peaks presented larger variation then in Fig.9b. It is possible that the greater peaks of force found in Fig. 9 (a) occur during the passage of the tooth in the austenite phase.



(a) Experiment 8.



(b) Experiment 2.

Fig. 9. Variation of the maximum cutting force x feed per tooth.

4.3. Tool wear

The increase of the cutting speed in machining processes tends to lower the life of the cutting tool because of the bigger wear. Consequently, the cutting force obtained with this tool tends to increase over time.

Figure 10 shows the raise of the specific cutting pressure for all the first, second and third replicas of all experiments. It is possible to observe the increase of the tool wear by the increase of the specific cutting

pressure.

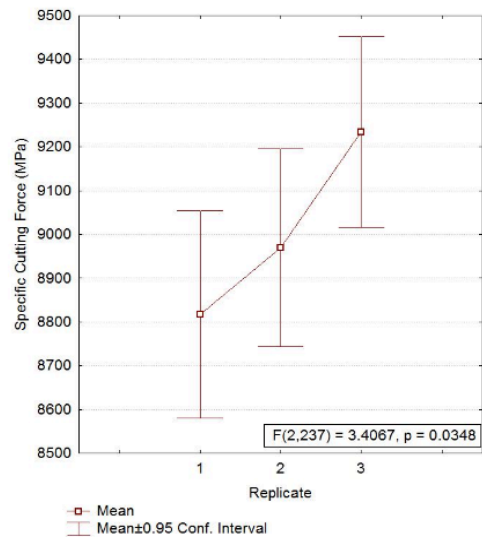


Fig. 10. Variation of the specific cutting pressure for the three replicas of all experiments.

Figure 11 presents the decrease of the specific cutting pressure when the tool works with bigger cutting speed. This fact can be due to the decrease of the deformation and the hardness of the chip, as well as the decrease of friction caused by the raise of the cutting speed [16]. Additionally, it is known, also, that the increase of the temperature during the machining of superduplex with high cutting speed tends to prevent the formation of built-up edge and, consequently, decrease the specific cutting pressure.

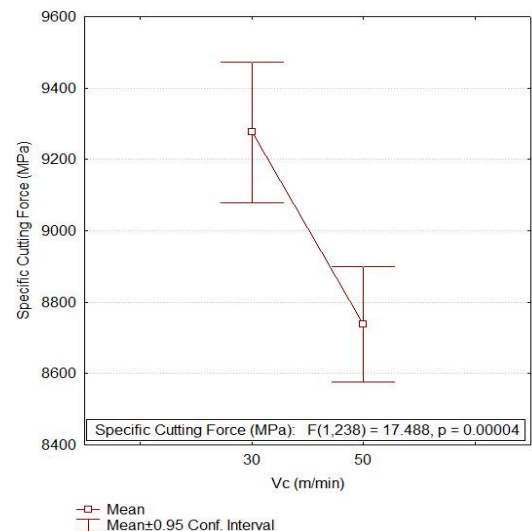


Fig. 11. Variation of the specific cutting pressure x cutting speed.

5. Conclusions

This article deals with micromilling of superduplex UNS S 32750 with two levels of feed per tooth and two levels of cutting speed, and constant depth of cut. A mechanistic model for the computation of the cutting force was used to calculate the specific cutting pressure. The model was calibrated with maximum error around 0.59%.

The increase of feed per tooth, as expected, decreased the specific cutting pressure. In other hand, a higher cutting speed reduces the specific cutting pressure due the increase of temperature in the cutting region that prevents the formation of built-up edge.

For the lower feed per tooth, $f_z=0.007$ mm/th, it is possible to observe a stronger variation of the force peaks, that could indicate the passage of each tooth in a unique phase at once.

Therefore, the superduplex is a good choice for the study of cutting force variation caused by a biphasic and chemically differentiated microstructure. The suggestion for future works is to decrease the feed per tooth (<0.007 mm/th) and depth of cut (<0.1 mm) values, so this supposition can be reinforced.

Acknowledge

The authors thanks to: the support of the CAPES for acquiring the equipment used in this article thru Pro-equipment resources and for the Mechanical Engineering Department. The cutting fluid was kindly supplied by Quaker Industries.

References

- [1] A. Aramcharoen et al., "Size effect and tool geometry in micromilling of tool steel". *Prec. Eng.*, 2009; V33: 402-407.
- [2] W.Y. Bao, I. N. Tansel, "Modeling micro-end-milling operations. Part I: analytical cutting force model", *Int. J. Mach. T. Manuf.*, 2000, V40: 2155-2173.
- [3] F. Vollertsen et al., "Size effects in manufacturing of metallic components", *CIRP Annals*, 2009; V58: 566-587.
- [4] M. Câmara et al., "State of the art on micro milling of materials, a review". *J. of Mat. Sci. & Tech.*, 2012; V28, No. 8: pp. 673 – 685.
- [5] S. M. Afazov et al., "Effects of micro milling conditions on the cutting forces and process stability". *J. of Mat. Proc. Tech.*, 2013; V213: 671-684.
- [6] A. Bayesteh et al., "2-Dimensional ploughing simulation model development in micro flat end milling". In 8th ICOMM, 2013. Victoria, Canada.
- [7] A. C. Ramos et al., "Characterization of the transition from ploughing to cutting in micro machining and evaluation of the minimum thickness of cut". *J. of Mat. Proc. Tech.*, 2012; V212, No. 3: 594 – 600.
- [8] M. P. Vogler et al., "On the modeling and analysis of machining performance in micro-endmilling, Part II: Cutting force prediction", *J. of Man. Sci. and Eng.*, 2004; V126: 695-705.
- [9] M. Malekian et al., "Modeling of minimum uncut chip thickness in micro machining of aluminum", *J. of Mat. Proc. Tech.*, 2012; V212: 553-559.
- [10] A. Simoneau et al., "Grain Size and Orientation

Effects When Microcutting AISI 1045 Steel", *CIRP Annals*, 2007; V56: 57-60.

[11] A. Simoneau et al., "Chip formation during microscale cutting of a medium carbon steel", *Int. J. Mach. T. Manuf.*, 2006; V46: 467-481.

[12] W. Kline et al., "The prediction of cutting forces in end milling with application to cornering cuts". *Int. J. of Mach. T. Des. and Res.*, 1982; V22, No. 1: 7 – 22.

[13] J. Tlustý and P. MacNeil, "Dynamics of cutting in end milling". *Annals of CIRP*, 1975; V24: 213 – 221.

[14] G. Newby et al., "Empirical analysis of cutting force constants in micro-end-milling operations". *J. of Mat. Proc. Tech.*, 2007; V192-193, No. 0; 41 – 47.

[15] X. Liu et al., "An analytical model for the prediction of minimum chip thickness in micromachining". *Trans. ASME*, 2006; V128: 474 – 481.

[16] M. Alauddin et al., "Cutting forces in the end milling of Inconel 718", *J. of Mat. Proc. Tech.*, 1998; V77: 153-159.